Submitted, accepted and published by
J. Environ. Monit., 2011, 13, 319-327

Characterization of PM10-bound polycyclic aromatic hydrocarbons in the ambient air of Spanish urban and rural areas

M. S. Callén*, J.M. López, A.M. Mastral

Instituto de Carboquímica (CSIC), Miguel Luesma Castán, 4, 50018 Zaragoza (Spain)

∗ Corresponding author. Phone number: +34 976 733977; Fax number: +34 976 733318

e-mail: marisol@icb.csic.es

Abstract

Urban areas constitute major pollution sources due to anthropogenic activities located in these areas. Among the legislated air pollutants, the particulate matter with an aerodynamic diameter less or equal than 10 microns (PM10) and polycyclic aromatic hydrocarbons (PAH) are controlled under Directive 2008/50/EC and Directive 2004/107/EC, respectively due to their adverse health effects.

A study was carried out at four urban and rural Spanish areas during the warm and cold seasons in 2008-2009 to quantify 19 PAH associated with the atmospheric PM10 by gas chromatography-mass spectrometry-mass spectrometry detection (GC-MS-MS) with the internal standard method.

The particle-bound composition of the analysed PAH was 5 and 10 times greater in industrial and urban areas, respectively when compared to those measured in rural areas. The highest PAH concentrations during the cold period were possibly due to the additional contribution of domestic heating sources and meteorological conditions such as low temperature and solar irradiation. The use of molecular diagnostic ratios indicated that the possible, major PAH pollution sources in the most polluted areas were pyrogenic sources, mainly attributed to

petroleum combustion sources (motor vehicle emissions, crude oil combustion). Petrogenic sources related to evaporative emissions also seemed to contribute in the most polluted area during the warm period. Those dates with high carcinogenic character according to the benzo(a)pyrene equivalent (BaP-eq) were also possibly attributed to petroleum combustion sources.

Keywords: PM10; PAH; air pollution; carcinogenic character; diagnostic ratios

Introduction

The air quality is an important factor that should be preserved mainly because the atmosphere is essential to support life on Earth. Sources of air pollution can be classified into two categories: anthropogenic sources and natural sources (wildfires, volcanic activity, dust from natural sources, etc). Anthropogenic sources include stationary sources such as factories, power plants and mobile sources like traffic, aircraft, chemicals, waste deposition, etc. Therefore, urban cities constitute one of the main air pollution sources. This justifies the need to assess the air quality regarding hazardous pollutants. A particular group of hazardous air pollutants are polycyclic aromatic hydrocarbons (PAH). These compounds, although emitted at low concentrations, are highly toxic and/or carcinogenic[1-3] and once released to the atmosphere can be deposited on soil and water affecting to different ecosystems. In addition, PAH can be supported onto the particulate matter and also can be in gas phase travelling long distances as a function of the meteorological conditions and their characteristics[4-6]. In this way, it cannot be assured that air pollution affects only urban and industrial areas but also rural areas can undergo pollution due to long-range transport.

The assessment of the air quality all around the world is essential in order to better understand the PAH atmospheric chemistry. Different studies have been carried out in different countries[7,8] trying to find out the main PAH pollution sources to achieve future abatements. In this work, four sampling places were chosen as representative of anthropogenic and non

anthropogenic PAH emission sources in order to know how different phenomena can affect the air quality in Aragón (Spain). PAH were studied at each sampling site regarding the ring size distribution, the particle-bound composition and the air pollution sources in order to get information that could be suitable for implementing corrective actions.

2. Experimental

2.1 Sampling program

Four monitoring sites corresponding to Zaragoza city ZGZ (41º39´49.38´´N; 0º53´16.68´´W) (urban area with traffic and industrial activities as main pollution sources)[9], Monzón city MON (41º53´59´´N; 0º10´47´´E) (urban background area with industry related to food, construction, chemicals and service sector), Monagrega (Teruel) MNG (40º56´23´´N; 00º19´15´´W) (regional background area situated 7.6 km from a power station of 1050 MW) and Torrelisa (Huesca) PIR (42º27´36´´N; 0º10´48´´E) (rural area representative of biogenic sources) were sampled during summer 2008 (23-05-2008 to 03-08-2008) and winter 2009 (13-01-2009 to 24-03-2009) according to previous bibliography[10] collecting a total of 30 samples for each place.

The sampling was performed with a GUV-15H Graseby Andersen High-Volume sampler with volumetric flow controlled system (1.13 m^3 min^{-1}) provided with a PM_{10} cut off inlet at 10 μm to capture PAH in the particle phase (PTFE-coated, glass-fibre filters, 0.6 μm pore size) during 24 h. More details regarding the sampling procedure and filters treatment have been previously published[11]. Briefly and previous to the sampling, filters were extracted by Soxhlet for 24 h with dichloromethane (DCM). Before and after sampling, the filters were equilibrated to constant temperature and relative humidity conditions for a minimum of 24 h prior to weighting. An analytical balance (precision of 0.01 mg) was used to obtain gravimetrically the particle mass and the PM10 concentrations were calculated by dividing the weight of the particulates captured on the filter by the air volume that passed through the sampler. After

sampling, filters were wrapped in aluminum foil, previously rinsed with hexane, and stored in a freezer at -20ºC until analysis.

2.2. Extraction and analyses

The PAH concentrations (phenanthrene (Phe), anthracene (An), 2+2/4 methylphenanthrene (2+2/4MePhe), 9 methylphenanthrene (9MePhe), 1-methylphenanthrene (1MePhe), 2,5-/2,7-/4,5-dimethylphenanthrene (DiMePhe), fluoranthene (Flu), pyrene (Py), benzo(a) anthracene (BaA), chrysene (Chry), benzo(b)fluoranthene (BbF), benzo(k)fluoranthene (BkF), benzo(e)pyrene (BeP), benzo(a)pyrene (BaP), indeno(1,2,3-cd)pyrene (IcdP), dibenz (a,h)anthracene (DahA), benzo(g,h,i)perylene (BghiP) and coronene (Cor)) were analyzed by GC-MS-MS with the internal standard method according to procedure previously published[11,12]. Briefly, the particle matter contained in the filters was extracted by Soxhlet during 18 h with DCM after the addition of deuterated-PAH surrogate standards containing the following PAH: anthracene- d_{10} (An-d_{10}), benzo(a)pyrene-d_{12} (BaP-d_{12}) and benzo(ghi)-perylene-d_{12} (BghiP-d_{12}). Extracts were concentrated on a rotary evaporator followed by a stream of nitrogen gas. Samples were cleaned-up through a silica gel column and eluted with DCM. Then the eluted sample was evaporated using a gentle nitrogen gas stream and the extract reconstituted with an internal standard solution (p-terphenyl) in hexane. PAH quantification was performed using the internal standard method relative to the closest eluting PAH surrogate.

2.3. Quality control and quality assurance

Analyses of four samples of an appropriate standard reference material (SRM 1649a, urban dust) provided by the National Institute of Standards and Technology (NIST) were carried out in order to check the analytical accuracy and precision. Measured values were comparable to certified values with the minimum relative errors for An (1%) and the maximum for Flu and Py 20% (Table S1, Supplementary data).

2.4. Statistical analysis

Statistical analysis of sample data was performed using the SPSS version 15.0 statistical package. In all cases, a probability of 0.05 or lower ($p \leq 0.05$) was considered as significant. Student´s t-tests of independent samples for each sampling site were carried out to evaluate differences in seasonal PAH concentrations. A precondition for this parametric test is to assess variance homogeneity through the Levene´s test. Pearson correlation coefficients were used to evaluate correlations between individuals PAH levels and PM10 for each sampling site.

2.5. Meteorological variables

The meteorological variables recorded for each sampling place were provided daily by the Estación Experimental de AULA-DEI (CSIC) and by the Aragon Government (DGA).

3. Results and discussion

3.1. PAH concentration and Seasonal evolution

The PAH concentration for each sampling place during the warm and cold seasons as well as the average concentrations for both seasons are shown in Table 1. In all these sampling places, the cold season favoured the accumulation of PAH registering the highest concentrations according to the following order: ZGZ>MON>MNG>PIR. The same decreasing order was also obtained during the warm season although with lower concentrations. ZGZ, the place corresponding to urban area, reasonably populated with high influence of anthropogenic activities, including industry and traffic, was the most polluted area followed by MON, urban background area slightly affected by industry and traffic sources. MNG and PIR showed the lowest PAH concentrations, more typical from regional and rural areas despite the presence of a power station localised in MNG as above mentioned. In fact, PIR is located in the Pyrenees Mountains with minimum anthropogenic PAH emissions. Therefore, the PAH concentrations in each sampling place were indicative of the pollution level of each place and they were

consistent with the locations of the sampling sites. According to Student´s t-test, these variations between seasons were only statistically significant at 95% level in ZGZ and MON indicating that pollution sources affecting both places were different during the cold and warm seasons. Meteorological factors such as low solar radiation could also favour the PAH increase during the cold season due to the lower photochemical decomposition. The additional anthropogenic sources related to domestic heating could be considered as responsible for the increase in PAH concentrations compared to warm season. This trend, of high PAH concentrations in cold season, has already been reported by other authors[13-15] and has been attributed to the above mentioned reasons.

The individual PAH which reached the highest concentrations, were IcdP+DahA (both compounds could not be separated in all samples) and BbjkF (∑BbF+BjF+BkF) in ZGZ, MON and PIR for both seasons. This predominance was also shown in previous studies carried out in urban and industrial areas in La Plata (Argentina) and Leipzig (Germany)[15]. IcdP, BbF and BkF are all indicators of vehicular emissions[14,16]. In MNG during the warm season Py and Chry, BbkF and BghiP were the predominant PAH. Phe, Flu and Py are characteristic of coal combustion which could reflect the impact of the power station localized in this place.

Because PAH include a wide range of compounds with different number of aromatic rings, properties and volatility, the PAH concentrations for each sampling place were classified according to rings number, from 3 to 7 rings, to study the PAH distribution pattern (Figure 1). Although in this work, PAH were only collected in the particulate phase and the concentrations of the most volatile PAH were almost negligible, it is interesting to know the PAH nature because PAH of high molecular weight are more carcinogenic than those of low molecular weight [17,18](Lu et al. 2008; Slezakova et al. 2009). It was found that independently of the sampling site, 4 rings PAH were the predominant PAH. In this group, Flu and Py are

included and these PAH are found in all combustion emissions[19]. It was possible to distinguish two different trends as a function of the pollution level. On the one hand, ZGZ and MON, the most polluted places showed lower percentage of 3 rings PAH and higher percentage of 7 rings PAH. On the other hand, MNG and PIR, the lowest polluted places decreased their percentage in heavy PAH (6-7 rings), increasing the 3 rings PAH. The major producers of heavy PAH are related to motor vehicle emissions, in particular petroleum driven cars, Cor and BghiP[20]. In addition, Cor has been found in urban areas with predominance of heavy-duty vehicles[8]. This could corroborate the higher traffic intensity in the urban and suburban areas corresponding to ZGZ and MON versus the rural areas MNG and PIR.

3.2. BaP concentration and carcinogenic character

One of the most interesting PAH to analyze is BaP which is an indicator of carcinogenic risk[21] and one of the compounds legislated according to European Directives[22]. The average BaP concentration in ZGZ was 0.283±0.391 ng m^{-3}, in MON 0.139±0.018 ng m^{-3}, in MNG was 0.033±0.023 ng m^{-3} and in PIR was 0.015±0.021 ng m^{-3} (Figure 2a)). The results found in ZGZ were similar to those found in Los Angeles, USA (0.21 ng m^{-3})[23] and slightly lower to the ones found in La Plata, Argentina (0.38 ng m^{-3})[24] and Las Palmas, Gran Canaria (0.34 ng m^{-3})[13]. Nevertheless, this PAH is not well representative of the carcinogenic character of the particulate matter because photodecomposition can reduce the BaP concentration and other PAH are also carcinogenic. This is the reason why the BaP equivalent (BaP-eq) was used by considering the toxic equivalent factors for different PAH. In this work, the Larsen and Larsen (1998) factors[25], which are the last reviewed, were used (Table S2, Supplementary data). Figure 2b) shows the results obtained of the BaP-eq for the different sampling sites during the warm and cold seasons. Independently of the season, ZGZ was the place with higher carcinogenic character regarding the BaP-eq and this character was higher during the cold season than the warm period. This higher contribution during cold season could be attributed

to low photochemical degradation, the higher impact of pollution sources with contribution of domestic heating and low temperatures which could favour the PAH accumulation. According to figure 2b), samples corresponding to 15th, 16th, 17th and 18th of January 2009 taken in ZGZ were the samples with the highest risk for human health. These dates were also coincident with the highest PM10 concentrations and were related to bonfires celebrated for San Juan festival during winter season and to the contribution of additional local pollution sources. Analysing the PAH that contributed more to the BaP-eq, it was observed that IcdP+DahA (ZGZ: 57%; MON: 59%, MNG: 38%; PIR: 44%) and BaP (ZGZ: 30%; MON: 29%; MNG: 48%; PIR: 19%) were the highest PAH contributors in terms of potential air carcinogenic activity independently of the sampling place. In this particular sampling, these results corroborated the importance of not only BaP as an indicator of humans' health risks but also other PAH as IcdP+DahA should also be considered in the evaluation of air quality in terms of PAH pollution as mentioned in Directive 2004/107/EC[22].

3.3. Particle-bound total PAH composition

In order to discard the influence of the PM10 on PAH concentrations, the particle-bound total PAH composition (μg g^{-1}) was also studied. It is defined as the PAH concentration normalized by the total particle mass collected. Figure 3 shows the temporal evolution of particle-bound total PAH composition for each sampling site during the warm and cold seasons. Regarding the warm season, the particle-bound composition followed a similar trend to the BaP-eq for each sampling site, with the highest concentration in ZGZ for the 02/06/2008. In the cold season it was observed that the trend was different to the BaP-eq distribution. Not only high particle-bound compositions were obtained for ZGZ but also for MON and MNG. In the case of ZGZ the two dates with the highest particle-bound PAH composition were 22/01/2009 (PM10=6.64 μg m^{-3}) and 14/01/2009 (PM10=24.36 μg m^{-3}). The previous dates mentioned in Section 3.2, 15th, 16th, 17th and 18th of January 2009 also had high particle-bound composition

although lower than the 14th and the 22nd of January 2009. High particle-bound PAH compositions were also obtained for the 13/02/2009 and 6/02/2009 in MON (both Friday), which corresponded to low PM10 concentrations of 4.54 and 2.53 μg m^{-3}, respectively and for the 05/03/2009 (PM10=17.14 μg m^{-3}) and 04/03/2009 (PM10=22.31 μg m^{-3}) in MNG. Therefore, the highest PAH concentrations were not always obtained for samples with the highest PM10 concentrations. Nevertheless, significant positive correlations at 99% level (Pearson correlation) between PM10 and total PAH concentrations and between PM10 and BaP were obtained for ZGZ (0.826 and 0.887) indicating that these pollutants originated from the same sources. A significant positive correlation was also obtained between PM10 and BaP for MON (0.470) so that ZGZ and MON followed the same trend regarding PM10 and BaP indicating that in both places, the highest the particulate matter the highest the carcinogenic character. MNG and PIR, the places with the lowest PAH pollution, did not follow this pattern, finding that in MNG long-range transport could be contributing to local pollution sources.

The average particle-bound total PAH compositions are also shown in Table 2 for each sampling place and for different seasons. It was observed that, independently of the PM10 concentration and sampling place, the PAH composition was higher in the cold season. A cold/warm ratio was also studied for each sampling site and it was more remarkable in MON and MNG while in ZGZ and PIR this ratio was only 3 and 2 times respectively greater during the cold season. In the case of PIR, the PAH influence was low as it could be expected in a place not directly influenced by anthropogenic sources while in the case of ZGZ this could be indicative of the low seasonality of pollution sources and the predominance of local pollution sources along the year. The higher PAH concentrations obtained during the cold season were probably due to the contribution of additional pollution sources like domestic heating and meteorological factors that could favour the PAH accumulation.

A new ratio was also studied for the different sampling places taking as reference or blank of pollution PIR, the lowest polluted area. The urban site, ZGZ showed a ratio 10 times greater than the rural area PIR and this ratio increased to 8 and 11 times, respectively for the warm and cold periods. The background urban area MON showed ratios twice and 6 times greater than the rural area for the warm and cold periods. Finally, the background rural area, MNG presented ratios 6 times greater than PIR for the cold season corroborating in this way, the pollution level of each sampling site.

3.4. Molecular ratios

One of the most important aspects to abate PAH pollution is to identify the pollution sources. To get this aim, molecular ratios between different PAH were studied for each sampling site according to bibliography[26-47] (Table 3). The results obtained for the different selected ratios for the four sampling sites and for both seasons are also shown in Table 3. It is noteworthy that these ratios only provide qualitative information and such information has to be processed with caution due to the difficulty in PAH sources discrimination and to some PAH reactivity. However, it can be used in a first step as a quick tool to identify the origin of PAH in ambient air.

PAH of molecular mass 178 and 202 are frequently used to distinguish between combustion and petroleum sources[26,27]. Thus, the An/(Phe+An) ratio <0.10 is usually taken as an indication of petroleum while a ratio >0.10 reflects the dominance of combustion sources[26].

For mass 202, a Flu/(Flu+Py) ratio of 0.50 is usually defined as the petroleum/combustion transition point[26] so that it is below 0.50 for most of the petroleum samples (fresh fuel oil, gasoline[28,31], diesel[28-32] combustion and crude oil combustion[33]) and above 0.50 in kerosene, grass, most coal and wood[34,35] combustion samples. However, this transition point seems to be closer to 0.40 than 0.50 so that ratios between 0.40 and 0.50 are more characteristic of petroleum combustion products (motor vehicle emissions and crude oil combustion)[27].

According to Table 3, the potential pollution sources in ZGZ and MON were associated with combustion sources such as crude oil[33], wood[34,35] and diesel[28-32] combustion, metal scrap burnt[36] or even road dust[37,47]. The influence of wood[34,35] and coal/coke combustion[38] for domestic heating could be reflected in PIR during the cold season. Figure 4a) shows the plots for the individual ratios of An/(Phe+An) versus Flu/(Flu+Py) for each sampling site during the warm and cold periods. Most of the samples in ZGZ, MON and PIR showed Flu/(Flu+Py) ratios higher than 0.4 (Figure 4a) and An/(An+Phe) ratios higher than 0.1 suggesting, as potential pollution sources, combustion sources related with petroleum combustion such as motor vehicle emissions. In the case of ZGZ, four samples corresponding to 24/05/2008, 30/05/2008, 03/06/2008 and 04/06/2008 (Fig. 4a) collected in the warm period seemed to indicate the influence of unburned fuel and evaporative emissions which could be mainly related to fuel evaporation during refuelling. In fact, around 300 m from the sampling point in ZGZ there were two petrol stations which could contribute to PAH concentrations especially in the warm period. For the less polluted areas: MNG and PIR, mixed petroleum and combustion sources were responsible of PAH concentrations. In MNG, this probably was explained by the presence of a coal power station that commonly uses fuel oil in addition to coal. Similar results were reported by Yunker et al.[27] (2002) in remote or light-urban samples suggesting mixed sources, with higher ratios in urban samples, as responsible of pollution sources. Evagelopoulos et al. [48] (2010) also indicated the presence of oil combustion sources in a heavy industrialized area and in an urban area in Greece (Flu/(Flu+Py)=0.45–0.48).

Yunker et al. [27] (2002) proposed that a ratio of BaA/(BaA+Chry) was indicative of petrogenic inputs, whereas ratios greater than 0.35 point to combustion sources. In ZGZ, MON and MNG, especially in the cold period, combustion sources (kerosene and wood combustion[32,34,35], coke furnaces[38], etc) were the predominant pollution sources (Table 3) while in PIR, the very low ratios of four rings PAH proved that this region was a non polluted

area like it could be expected by its localization. Figure 4b) shows the plots between the BaA/(BaA+Chry) versus the Flu/(Flu+Py) ratios for the four sampling sites. It was observed that most of the samples with BaA/(BaA+Chry) ratios higher than 0.35 corresponded to Flu/(Flu+Py) ratios higher than 0.4 indicating that combustion products are an important source of the most polluted samples like it was reflected in ZGZ, MON and MNG. In ZGZ, a few samples corresponding to the warm season were attributed to petroleum sources, probably due to evaporative emissions. These samples with low BaA/(BaA+Chry) ratios also suggested significant photolytic losses of BaA, which could be attributed to the higher solar radiation, to the higher temperature and to the higher photolytic decomposition typical of the warm season.

A very interesting ratio which gives us information on the unburned fossil fuels in the air is the ∑MePhe/Phe ratio[32,39,40]. The predominance of alkylated PAH is related to petrogenic (unburned petroleum products) sources[27,39], whereas the predominance of non-substituted or parent PAH is from pyrogenic (combustion of biomass and fossil fuels) origin. ZGZ and MON showed similar mean ratios (Table 3) with higher ratios in summer consistent with a greater contribution from unburned fossil fuel (e.g., evaporative losses during fuel refuelling and/or evaporation of fossil fuel drippings) that can be significant in urban areas. This relative abundance of MePhe isomers, slightly higher during the warm season than the cold season was already reported by Li et al.[39] (2009) in urban and suburban highway sites especially for diesel emissions. MNG also showed similar values to the ones found in ZGZ and MON in the cold period. A different trend was observed in the warm period in MNG with influence of petrogenic origin which was not reflected in the ∑MePhe/Phe ratio. This could probably be attributed to the power station localised in the surroundings of the sampling point in MNG. In fact, this ∑MePhe/Phe ratio value in the warm period was more similar to the ones reported by Simo et al.[40] (1997) in coal power plant aerosols after suntest irradiation (0.2). Other ratios that have also been applied to distinguish between pyrogenic and petrogenic PAH sources[33]

are Phe/An[26] and Flu/Py[26] (Table 3). The PAH of petrogenic origin prevalent in coals and fossil fuels mainly consist of low molecular weight PAH whereas the pyrolytic PAH consist mainly of four or more aromatic rings. Thus, an increase in higher molecular weight PAH, like it happened in ZGZ and MON, is indicative of pyrolytic origin PAH. Phe/An ratios of 1-10 have been reported by Budzinski[26] for PAH of pyrolytic origin as well as Flu/Py ratios between 1 and 2. Figure 4c) shows the plots of Flu/(Flu+Py) versus Phe/An for each individual sample and place. Most of the samples had pyrolytic origin related to petroleum combustion sources. Nevertheless and as it was mentioned previously, in ZGZ there were four samples not related to combustion sources during the warm season that although they did not have a proper petrogenic origin were due to petroleum sources (evaporative emissions).

According to Li and Kamens[28], other ratio that provides information regarding pollution sources is the BaA/BaP ratio. A ratio of 0.5 is indicative of gasoline combustion emissions while a ratio equal to the unity is considered like diesel and wood combustion so that diesel vehicles emissions and wood combustion were potential pollution sources (Table 3) for all sampling sites with the exception of PIR. Figure 4d) shows the plots between BaA/BaP and Flu/(Flu+Py) ratios for each individual sample that corroborate these results.

The BeP/(BaP+BeP) ratio presented similar values for the mean, warm and cold periods in ZGZ. This indicated on the one hand, the presence of road dust[37] and industrial furnaces[43] (Table 3) and on the other hand, the lack of seasonality and the predominance of local pollution sources. In MON and MNG, these ratios were also related to wood combustion[28] and road dust[47]. The faster decay of BaP in comparison to the more stable isomer BeP was more evident at PIR, MNG and MON during the warm season indicating possible PAH transport from distant sources. The BaP/BghiP ratio was also indicative of diesel emissions in all the four places[41].

Finally, it was very interesting to know the main pollution sources for those samples of ZGZ presenting the highest carcinogenic character calculated according to the BaP-eq and to the particle-bound PAH composition. It was observed that pyrolytic sources associated to petroleum combustion sources, more exactly to motor vehicle emissions, were the most dangerous pollution sources for population in all plots (Figure 4a-4d).

4. Conclusions

Results obtained in this work showed the pollution level with regard to PAH in four sampling places in Spain. This pollution level was related with the anthropogenic activities developed in each place, following the decreasing order: ZGZ>MON>MNG>PIR with maximum PAH concentrations in the urban place and minimum in the rural area. The meteorological conditions typical of the cold season favoured the PAH concentration in all sampling sites, implying high risk for human health. In fact, the samples which should have the highest carcinogenic character according to the BaP-eq were found during this cold period in the most polluted area ZGZ. PAH of high rings (6-7) were prevalent in the most polluted areas, ZGZ and MON, while low rings PAH (3-4) increased in the least polluted areas, MNG and PIR.

Molecular ratios allowed discerning the main potential pollution sources, in three of the four sampling sites: ZGZ, MON and MNG. These sources had pyrolytic origin and could be related to petroleum combustion sources associated with vehicular emissions, mainly diesel, coal, wood combustion and industrial furnaces. Samples with the highest risk for human health, according to the BaP-eq, would have also pyrolytic origin and could be mainly due to diesel traffic emissions. Additional pollution sources with petrogenic origin were also found in ZGZ during the warm season and they were related to evaporative emissions.

Acknowledgements

Authors would like to thank Aula Dei-CSIC (R. Gracia), the Government of Aragon (DGA), the Fondo Social Europeo de Desarrollo Regional and the Ministry of Science and Innovation for supporting the project CGL2009-14113-C02-01 and the Ramón y Cajal contract of J.M.L.

5. References

1. B. Binkova and R.J. Sram, *Mutat. Res.,* 2004, **547**, 109–121.
2. H. Rubin, *Carcinogenesis,* 2001, **2**, 1903–1930.
3. P.E.T. Douben, PAHs: An Ecotoxicological Perspective, Wiley, New York, 2003.
4. J.S. Park, L.T. Wade and S. Sweet, *Atmos. Environ.,* 2001, **35**, 3241-3249.
5. N. Vardar and K.E. Noll, *Environ. Monit. Assess.,* 2003, **87**, 81-92.
6. Y. Tasdemir and F. Esen, *Atmos. Environ.,* 2007, **41**, 1288-1301.
7. K. Saarnio, M. Sillanpa, R. Hillamo, E. Sandell, A.S. Pennanen and R.O. Salonen, *Atmos.Environ.,* 2008, **42**, 9087–9097.
8. A.M. Mastral, J.M. López, M.S. Callén, T. García, R. Murillo and M.V. Navarro, Sci. Total Environ., 2003, **307**, 111-124.
9. J.M. López, M.S. Callén, R. Murillo, T. Garcia, M.V. Navarro, M.T. de la Cruz and A.M. Mastral, *Environ. Res.,* 2005, **99**, 58-67.
10. M.S. Callén, J.M. López and A.M. Mastral, *J. Hazard. Mater.,* 2010, **180**, 648-655.
11. M.S. Callén, M.T. de la Cruz, J.M. López, R. Murillo, M.V. Navarro and A.M. Mastral, *Water Air Soil. Poll.,* 2008, **190**, 1-4.
12. M.S. Callén, M.T. de la Cruz, J.M. López, R. Murillo, M.V. Navarro and A.M. Mastral, *Chemosphere*, 2008, **73**, 1357-1365.
13. A.V. Castellano, J.L. Cancio, P.S. Alemán and J.S. Rodríguez, *Environ. Int.*, 2003, **29**, 475–80.
14. H. Guo, S.C. Lee, K.F. Ho, X.M. Wang and S.C. Zou, *Atmos. Environ.,* 2003, **37,** 5307–5317.
15. M. Rehwagen, A. Mqller, T.L. Massolo, O. Herbarth and A. Ronco, *Sci. Total Environ.*, 2005, **348**, 199–210.
16. P. Kulkarni and C. Venkataraman, *Atmos. Environ.,* 2000, **34**, 2785–2790.
17. H. Lu, L. Zhu and S. Chen, *Environ. Pollut.*, 2008, **152**, 569-575
18. K. Slezakova, D. Castro, M.C. Pereira, S. Morais, C. Delerue-Matos and M.C. Alvim-Ferraz , *Atmos. Environ.,* 2009, **43**, 6376–6382.
19. P. Masclet, G. Mouvier and K. Nikolaou, *Atmos. Environ.*, 1986, **20**, 439-446.
20. B. Zielinska, J. Sagebiel, J.D. McDonald, K. Whitney and D.R. Lawson, *J. Air Waste Manage. Assoc.*, 2004, **54**, 1138-1150.
21. WHO World Health Organization. Guidelines for air quality chapter 3, health-based guidelines. Geneva7 WHO; 2000. p. 32–71.
22. Directive 2004/107/EC of the European Parliament and of the Council of 15 December 2004 relating to arsenic, cadmium, mercury, nickel and PAH in ambient air.
23. B.C. Panther, M.A. Hooper and N. Tapper, *Atmos. Environ.,* 1999, **33**, 4087– 99.
24. C. Venkataraman, J.M. Lyons and S. Fiedlander, *Environ. Sci. Technol.*, 1994, **28**, 535–62.
25. J.C. Larsen and P.B. Larsen, Chemical carcinogens, in: R.E. Hester, R.M. Harrison (Eds.), Air Pollution and Health, Royal Society of Chemistry, Cambridge, UK, 1998, pp. 33–56.

26. H. Budzinski, I. Jones, J. Bellocq, C. Pierard and P. Garrigues, *Marine Chem.,* 1997, **58**, 85–97

27. M.B. Yunker, R.W. Macdonald, R. Vingarzan, R.H. Mitchell, D. Goyette and S. Sylvestre, *Org. Geochem.,* 2002, **33**, 489–515.

28. C.K. Li and R.M. Kamens, *Atmos. Environ.,* 1993, **27,** 523–32.

29. R.N. Westerholm, A. Christensen, M. Törnqvist, L. Ehrenberg, U. Rannug, M. Sjögren, J. Rafter, C. Soontjens, J. Almén and K. Grägg, *Environ. Sci. Technol.,* 2001, **35,** 1748–1754.

30. S.A. Wise, L.R. Hilpert, R.E. Rebbert, L.C. Sander, M.M. Schantz, S.N. Chesler and W.E. May, *Fresenius J. Anal. Chem.,* 1998, **332**, 573–582.

31. W.F. Rogge, L.M. Hildemann, M.A. Mazurek, G.R. Cass and B.R.T. Simoneit, *Environ. Sci. Technol.,* 1993, **27,** 636–651.

32. M. Sjögren, H. Liu, U. Rannug and R. Westerholm, *Environ. Sci. Technol.*, 1996, **30**, 38-49.

33. B.A. Benner, N.P. Bryner, S.A. Wise, G.H. Mulholland, R.C. Lao and M.F. Fingas, *Environ. Sci. Technol.,* 1990, **24**, 1418–1427.

34. J.J. Schauer, M.J. Kleeman, G.R. Cass and B.R. Simoneit, *Environ. Sci. Technol.,* 2001, **35**, 1716–1728.

35. P.M. Fine, G.R. Cass and B.R. Simoneit, *Environ. Sci. Technol.*, 2001, **35**, 2665–2675.

36. J-H. Tsai, B-H. Peng, S-T. Lin and D-Z. Lee, *Sci. Total Environ.*, 1995, **164**, 9–17.

37. S.G. Wakeham, C. Schaffner and W. Geiger, *Geochim. Cosmochim. Acta*, 1980, **44**, 403–413.

38. M.A. Sicre, J.C. Marty, A. Saliot, X. Aparicio, J. Grimalt and J. Albaigés, *Atmos. Environ.,* 1987, **21**, 2247–2259.

39. Z. Li, E.N. Porter, A. Sjödin, L.L. Needham, S. Lee, A.G. Russell and J.A. Mulholland, *Atmos. Environ.,* 2009, **43**, 4187–4193

40. R. Simo, J.O. Grimalt and J. Albaiges, *Environ. Sci. Technol.*, 1997, **31**, 2697–2700.

41. M.F. Simcik, S.J. Eisenreich and P.J. Lioy, *Atmos. Environ.,* 1999, **33**, 5071 5079.

42. M.P. Fraser, G.R. Cass, B.R. Simoneit and R.A. Rasmussen, *Environ. Sci. Technol.,* 1998, **32**, 1760–1770.

43. H.H. Yang, W.J. Lee, S.J. Chen and S.O. Lai, *J. Hazard. Mater.*, 1998, **60**, 159–174.

44. A.M. Caricchia, S. Chiavarini and M. Pezza, *Atmos. Environ.,* 1999, **33**, 3731-3738.

45. P. Masclet, M.A. Bresson and G. Mouvier, *Fuel,* 1987, **66**, 556–562.

46. J.M. Daisey, I. Hawryluk, T.J. Kneip and F. Mukai, Mutagenic activity in organic fractions of airborne particulate matter. In: T. Novakov, Editor, Conference on Carbonaceous Particles in the Atmosphere Natl. Techn. Inform. Serv., U.S. Dept. of Commerce (1979), pp. 187–192.

47. F. Rogge, L.M. Hildemann, M.A. Mazurek, G.R. Cass and B.R.T. Simoneit, Environ. Sci. Technol., 1993, **27**, 1892–1904.

48. V. Evagelopoulos, T.A. Albanis, EI. Kodona and S. Zoras, *Chemosphere,* 2010, **80**, 235-240.

Table 1. Mean individual PAH concentrations (ng m^{-3}), mean total PAH concentrations (ng m^{-3}) and mean total PM10 concentrations (μg m^{-3}) at each sampling place: ZGZ, MON, MNG and PIR during the warm and cold periods (n= sample size; standard deviations in brackets).

	Warm period				Cold period			
PAH	**ZGZ n=15**	**MON n=15**	**MNG n=15**	**PIR n=15**	**ZGZ n=15**	**MON n=16**	**MNG n=15**	**PIR n=14**
Phe	0.071 (0.090)	0.035 (0.021)	0.030 (0.043)	<l.d.	0.27 (0.13)	0.19 (0.072)	0.048 (0.043)	0.046 (0.010)
An	0.015 (0.013)	<l.q.	<l.q.	0.010 (0.01)	0.040 (0.030)	0.022 (0.015)	<l.q.	<l.q.
2+2/4 MePhe	0.035 (0.028)	<l.q.	<l.d.	<l.d.	0.063 (0.040)	0.040 (0.012)	0.012 (0.013)	0.013 (0.007)
9 MePhe	0.032 (0.024)	0.011 (0.004)	<l.d.	<l.d.	0.061 (0.044)	0.038 (0.014)	0.012 (0.012)	<l.q.
1 MePhe	0.042 (0.031)	0.011 (0.009)	0.022 (0.038)	<l.d.	0.082 (0.059)	0.046 (0.011)	<l.q.	<l.q.
DiMePhe	0.080 (0.067)	0.068 (0.18)	<l.d.	<l.d.	0.14 (0.13)	0.041 (0.023)	<l.q.	<l.q.
Flu	0.13 (0.11)	0.092 (0.026)	0.030 (0.043)	<l.d.	0.54 (0.45)	0.44 (0.262)	0.092 (0.078)	0.056 (0.016)
Py	0.18 (0.13)	0.10 (0.030)	0.040 (0.090)	<l.d.	0.63 (0.50)	0.44 (0.15)	0.097 (0.074)	0.055 (0.016)
BaA	0.11 (0.13)	0.043 (0.024)	0.029 (0.030)	<l.d.	0.73 (0.82)	0.38 (0.20)	0.048 (0.024)	<l.q.
Chry	0.24 (0.21)	0.090 (0.034)	0.041 (0.039)	0.020 (0.024)	0.81 (0.74)	0.48 (0.16)	0.074 (0.042)	0.046 (0.016)
BbjkF	0.27 (0.29)	0.17 (0.082)	0.030 (0.040)	0.027 (0.045)	1.6 (1.5)	0.87 (0.42)	0.13 (0.084)	0.066 (0.038)
BeP	0.097 (0.061)	<l.d.	0.015 (0.022)	<l.d.	0.52 (0.53)	0.27 (0.085)	0.033(0.023)	<l.q.
BaP	0.089 (0.075)	0.050 (0.018)	0.022 (0.023)	0.010 (0.022)	0.48 (0.48)	0.22 (0.079)	0.043 (0.023)	<l.q.
IcdP+DahA	0.46 (0.41)	0.23 (0.27)	0.018 (0.021)	<l.d.	1.4 (1.4)	0.90 (0.39)	0.10 (0.089)	0.087 (0.047)
BghiP	0.21 (0.14)	<l.d.	0.025 (0.023)	<l.d.	0.62 (0.41)	0.31 (0.13)	0.083 (0.050)	<l.q.
Cor	0.20 (0.15)	0.069 (0.11)	<l.d.	<l.d.	0.39 (0.35)	0.27 (0.14)	0.015 (0.034)	<l.q.
Mean total PAH	2.3 (1.5)	1.1 (0.62)	0.33 (0.47)	0.10 (0.12)	8.4 (7.2)	5.0 (1.6)	0.81 (0.53)	0.46 (0.18)

Mean total PM10	21 (5.5)	33 (5.7)	17 (6.7)	10 (7.4)	30 (21)	37 (12)	6.7 (5.3)	19 (6.2)

l.d.= the detection limit; l.q.= the quantification limit

Table 2. Mean particle-bound composition of PAH (μg g^{-1}) obtained by dividing the total PAH concentration by the PM10 during the warm and cold seasons at the four sampling places: ZGZ, MON, MNG and PIR. Mean particle-bound composition of PAH (μg g^{-1}) for both seasons at each sampling place. Cold/warm ratio and place/PIR ratio (taking PIR as non polluted area) of the PAH particle-bound composition for each sampling place (n= sample size).

	PAH			
	ZGZ μg g^{-1}	**MON μg g^{-1}**	**MNG μg g^{-1}**	**PIR μg g^{-1}**
Warm season	105 (n=15)	32 (n=15)	16 (n=15)	13 (n=15)
Cold season	288 (n=15)	151 (n=16)	144 (n=15)	26 (n=14)
Mean both seasons	196 (n=30)	93 (n=31)	80 (n=30)	19 (n=29)
Ratio Cold/Warm	3	5	9	2
Ratio Place/PIR	10	5	4	

Table 3. Mean molecular ratios used to discern potential pollution sources found in the four sampling sites: ZGZ, MON, MNG and PIR during the warm and the cold seasons and in the bibliography (n=sample size).

	An/(Phe+An)	Flu/(Flu+Py)	BaA/(BaA+Chry)	∑MePhe/Phe	Phe/An	Flu/Py	BaA/BaP	BeP/(BeP+BaP)	BaP/BghiP
ZGZ n=30	0.30	0.43	0.34	0.83	6.81	0.80	1.37	0.52	0.68
Warm (n=15)	0.49	0.40	0.26	0.91	5.23	0.75	1.32	0.54	0.72
Cold (n=15)	0.12	0.46	0.42	0.74	8.39	0.84	1.43	0.50	0.65
MON n=31	0.12	0.49	0.37	0.80	7.88	0.96	1.28	0.43	0.50
Warm (n=15)	0.15	0.48	0.31	0.89	6.51	0.94	0.83	0.30	0.15
Cold (n=16)	0.10	0.49	0.42	0.72	9.17	0.98	1.71	0.55	0.84
MNG n=30	0.04	0.31	0.37	0.61	3.13	0.60	1.55	0.34	0.66
Warm (n=15)	0.01	0.14	0.34	0.43	0.26	0.29	1.59	0.29	0.75
Cold (n=15)	0.07	0.48	0.40	0.79	6.01	0.92	1.50	0.40	0.58
PIR n=29	0.53	0.24	0.02	0.24	3.13	0.50	0.04	0.25	0.63
Warm (n=15)	0.93	n.d.	0.01	n.d.	n.d.	n.d.	0.02	0.07	0.56
Cold (n=14)	0.10	0.51	0.03	0.50	6.49	1.03	0.06	0.45	0.71
	An/(Phe+An)	**Flu/(Flu+Py)**	**BaA/(BaA+Chry)**	**∑MePhe/Phe**	**Phe/An**	**Flu/Py**	**BaA/BaP**	**BeP/(BeP+BaP)**	**BaP/BghiP**
Combustion									
Gasoline	0.11 [28 31]	0.44[28,31]	0.33-0.38[28,31]	<1[39]			0.5[28]	0.6-0.8[31]	1.3/0.3-0.4[45]
Diesel	0.11±0.05 [28-32] (0.01-0.27)	0.39±0.11 (0.20–0.58) [28-32],	0.38±0.11 (0.18–0.69) [28-32],	>1[39]			1[28] 0.85[44]	0.70[31]	0.5-0.8[41]
Wood comb.	0.19±0.04[34,35] (0.14-0.29)	0.51±0.06 (0.41–0.67) [34,35]	0.46±0.06 (0.30-0.54) [34,35]				1[28]	0.34[28]	
Kerosene comb.	0.14±0.02[32] (0.12-0.16)	0.50 [32]	0.37 (0.30-0.44) [32]						
Coal tar comb. (SRM1597)	0.18[30]	0.58[30]	0.54[30]						
Coal/coke comb.		0.52[38]	0.48+0.09 [38]				0.9-6.6 [46]		0.9-6.6 [46]
Coke furnaces		0.57±0.06 [38]	0.43+0.05 [38]						
Industrial furnaces		0.21-0.26 [43]						0.17-0.48 [43]	
Metal scrap burn		0.45 [36]	0.28[36]						
Crude oil comb.	0.22[33]	0.44±0.02 (0.42-0.46) [33]	0.49±0.01 [33] (0.470.50)						
Environmental samples									
Urban air (SRM 1648 and 1649a; n=3) [36,42]	0.08±0.02[a, 30,42] (0.06–0.09)	0.56±0.01 [a, 30,42] (0.55-0.57)	0.30±0.05 [a, 30,42] (0.24–0.33)						
Road dust	0.18[37,47]	0.42[37,47]	0.13[37,47]					0.54[47]	
Pyrogenic origin					1-10[26]	1-2[26]			

a NIST SRM 1649a certificate of analysis;
n.d.= not determined.

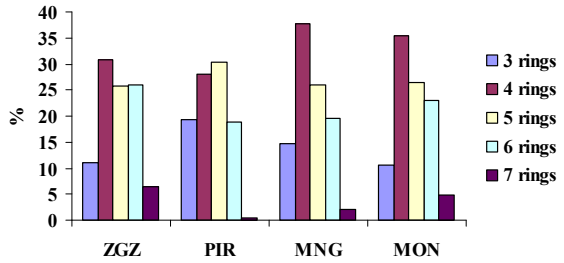

Figure 1. Percentage of ring PAH distribution as a function of the sampling place: ZGZ, PIR, MNG and MON (n= sample size; n=30 for ZGZ, n=29 for PIR, n=30 for MNG and n=31 for MON).

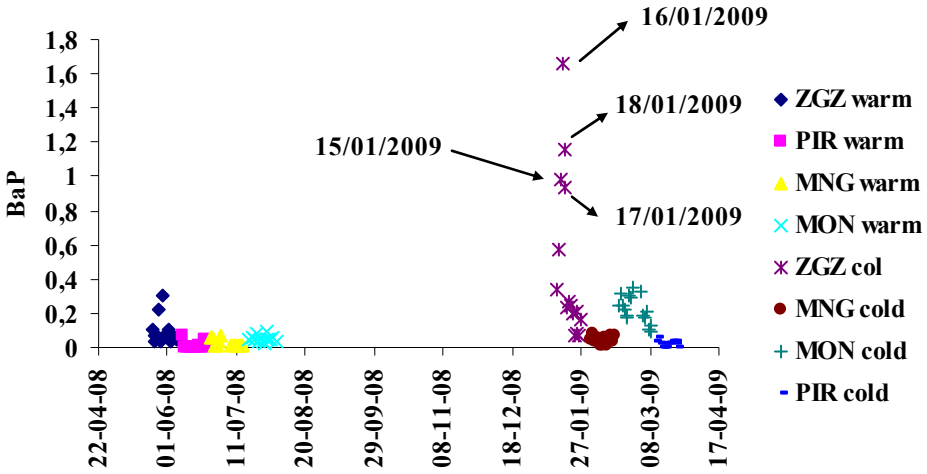

a)

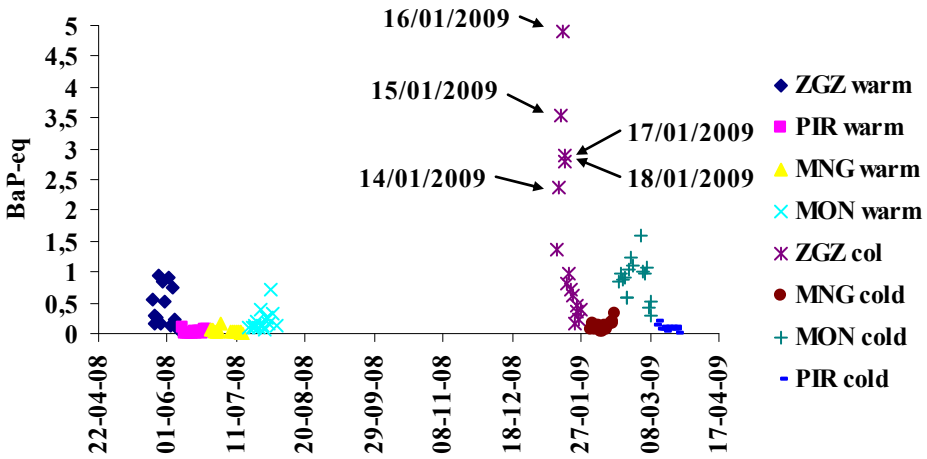

b)

Figure 2. Temporal evolution of a) BaP (ng m^{-3}) and b) BaP equivalents (ng m^{-3}) calculated with the Larsen and Larsen toxic equivalent factors for the four sampling sites: ZGZ, MON, MNG, PIR during the warm and the cold seasons (n= sample size; n=15 for ZGZ warm, n=15 for ZGZ cold, n= 15 for MNG warm, n= 15 for MNG cold, n=15 for MON warm, n=16 for MON cold, n=14 for PIR warm, n=15 for PIR cold)(TEF BaP=1).

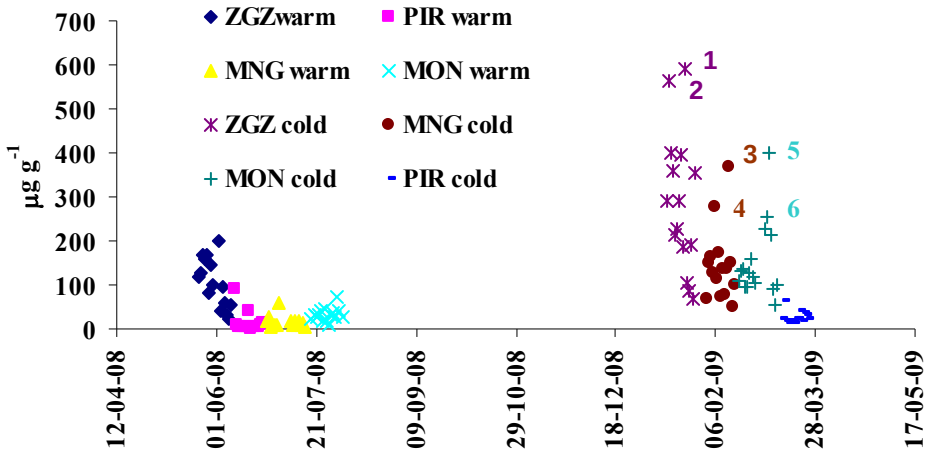

1. 22/01/2009
2. 14/01/2009
3. 13/02/2009
4. 06/02/2009
5. 05/03/2009
6. 04/03/2009

Figure 3. Temporal evolution of the particle-bound composition (µg g^{-1}) of PAH during the warm and cold seasons for each sampling place (ZGZ, MON, MNG, PIR) (n= sample size; n=15 for ZGZ warm, n=15 for ZGZ cold, n= 15 for MNG warm, n= 15 for MNG cold, n=15 for MON warm, n=16 for MON cold, n=15 for PIR warm, n=14 for PIR cold). Numbers 1 to 6 correspond to the following dates: 1. 22/01/2009; 2. 14/01/2009; 3. 13/02/2009; 4. 06/02/2009; 5. 05/03/2009 and 6. 04/03/2009.

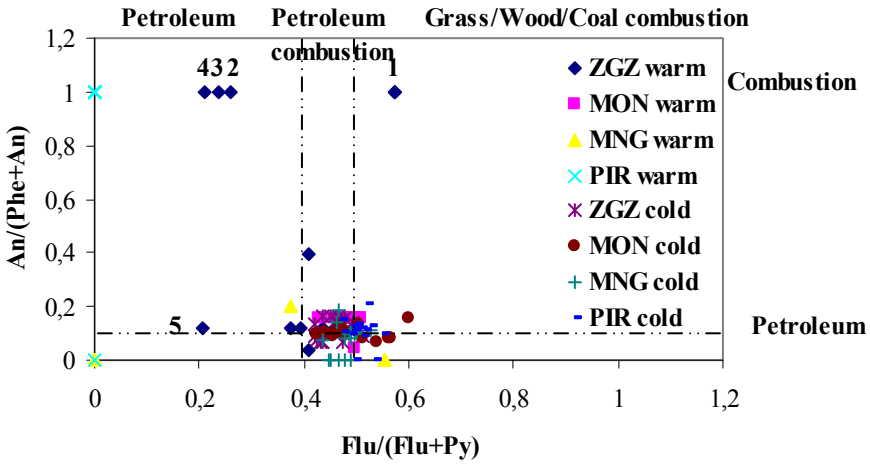
Petroleum
Petroleum combustion
Grass/Wood/Coal combustion
An/(Phe+An)
Flu/(Flu+Py)
1,2
1
0,8
0,6
0,4
0,2
0
0
0,2
0,4
0,6
0,8
1
1,2
4 3 2
1
5
ZGZ warm
MON warm
MNG warm
PIR warm
ZGZ cold
MON cold
MNG cold
PIR cold
Combustion
Petroleum

a)

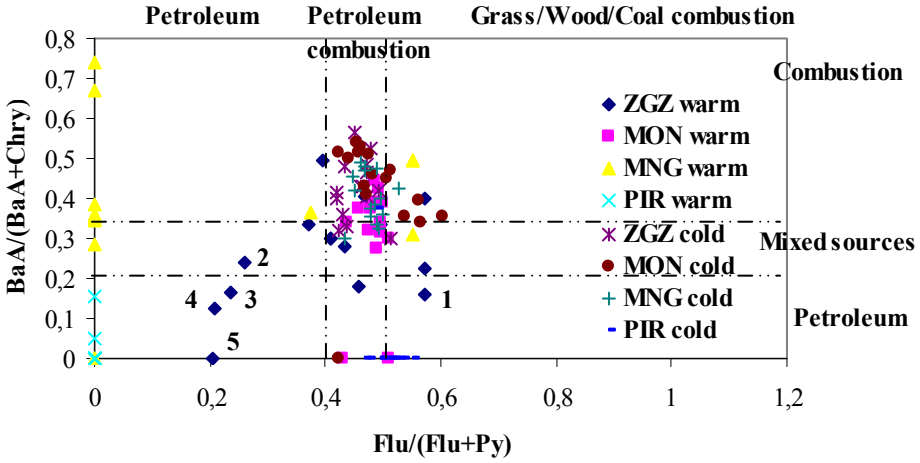
Petroleum
Petroleum combustion
Grass/Wood/Coal combustion
BaA/(BaA+Chry)
Flu/(Flu+Py)
0,8
0,7
0,6
0,5
0,4
0,3
0,2
0,1
0
0
0,2
0,4
0,6
0,8
1
1,2
2
4
3
1
5
ZGZ warm
MON warm
MNG warm
PIR warm
ZGZ cold
MON cold
MNG cold
PIR cold
Combustion
Mixed sources
Petroleum

b)

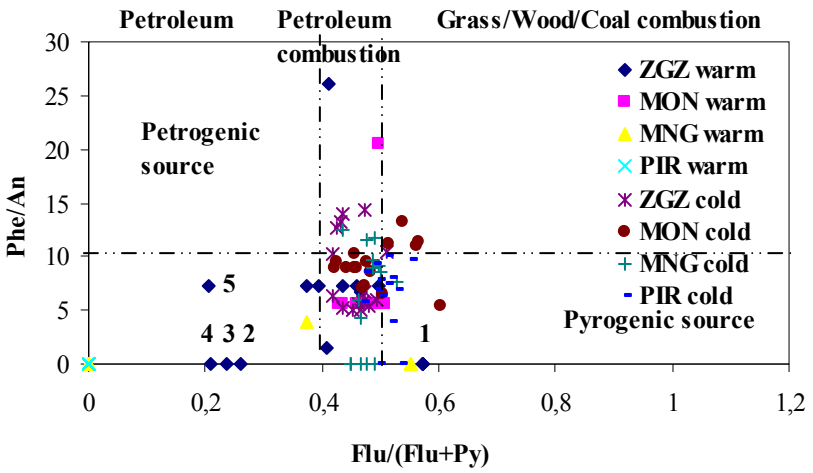

c)

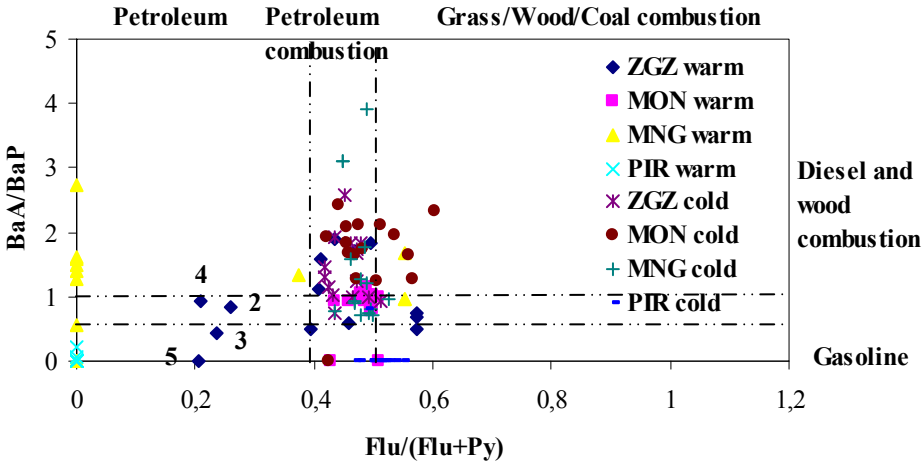

d)

Figure 4. Scatter plots of selected PAH molecular ratios for source discrimination in the four sampling places: ZGZ, MON, MNG and PIR during the warm and cold seasons where a) An/(An+Phe) versus Flu/(Flu+Py), b) BaA/(BaA+Chry) versus Flu/(Flu+Py), c) Phe/An versus Flu/(Flu+Py) and d) BaA/BaP versus Flu/(Flu+Py) (n= sample size; n=15 for ZGZ warm, n=15 for ZGZ cold, n= 15 for MNG warm, n= 15 for MNG cold, n=15 for MON warm, n=16 for MON cold, n=15 for PIR warm, n=14 for PIR cold). Numbers 1 to 5 correspond to the following dates: 1: 08/06/2008; 2: 03/06/2008; 3: 04/06/2008; 4: 24/05/2008; 5: 30/05/2008.